Journal of Statistical Physics, Vol. 95, Nos. 5/6, 1999

Singular Limit of a Reaction-Diffusion Equation with a Spatially Inhomogeneous Reaction Term*

K.-I. Nakamura,[1] H. Matano,[2] D. Hilhorst,[3] and R. Schätzle[4]

Received September 22, 1998; final January 25, 1999

We study reaction-diffusion equations with a spatially inhomogeneous reaction term. If the coefficient of these reaction term is much larger than the diffusion coefficient, a sharp interface appears between two different phases. We show that the equation of motion of such an interface involves a drift term despite the absence of drift in the original diffusion equations. In particular, we show that the same rich spatial patterns observed for a chemotaxis-growth model can be realized by a system without a drift term.

KEY WORDS: Reaction-diffusion equations; nonlinear diffusion; singular perturbation; interface motion; chemotaxis; matched asymptotic expansion.

1. INTRODUCTION

It is well-known that some classes of nonlinear diffusion equations give rise to sharp internal layers (or interfaces) when the diffusion coefficient is very small or the reaction term is very large. And the motion of such interfaces is often driven by their curvature. In this paper we consider a diffusion equation with a spatially inhomogeneous reaction term of the form

$$\varepsilon u_t = \varepsilon \nabla^2 u - \frac{1}{\varepsilon} h(x)^2 W'(u) \tag{1.1}$$

[1] Department of Computer Science and Information Mathematics, University of Electro-communications, 1-5-1 Chofugaoka, Chofu, Tokyo 182, Japan.
[2] Graduate School of Mathematical Sciences, University of Tokyo, 3-8-1 Komaba, Tokyo 153, Japan.
[3] Analyse Numérique et EDP, CNRS, et Université de Paris-Sud, 91405 Orsay, France.
[4] Mathematisches Institut der Albert-Ludwigs-Universität Freiburg, D-79104 Freiburg, Germany.
* Dedicated to Professor John W. Cahn on the occasion of his seventieth brithday.

0022-4715/99/0600-1165$16.00/0

where the parameter ε is sufficiently small and $W(u)$ is a double-well potential of equal well-depth. A typical example is $W(u)=u^2(1-u)^2$. Interestingly, the interface motion arising from the above equation involves not only a curvature term but also a drift term, despite the fact that no drift term is present in the original diffusion equation. More precisely we will prove that the interface motion for the above equation is identical to that for the equation

$$\varepsilon u_t=\varepsilon\nabla^2 u+\frac{\varepsilon}{h(x)}\nabla h(x)\cdot\nabla u-\frac{1}{\varepsilon}W'(u) \tag{1.2}$$

We will also study systems of equations without a drift term:

$$\begin{cases}\varepsilon u_t=\varepsilon\nabla^2 u+\dfrac{1}{\varepsilon}h(v)^2 f_\varepsilon(u), & x\in\mathbf{R}^N,\quad t>0\\ \varepsilon v_t=\nabla^2 v+u-\gamma v, & x\in\mathbf{R}^N,\quad t>0\end{cases} \tag{1.3}$$

and compare their interface motion with those with a drift term, such as a variant of the chemotaxis model proposed by Mimura and Tsujikawa[19] (see also ref. 20), namely

$$\begin{cases}\varepsilon u_t=\varepsilon\nabla^2 u-\varepsilon\nabla\cdot(u\nabla\chi(v))+\dfrac{1}{\varepsilon}f_\varepsilon(u) & \text{in } \Omega\times(0,T]\\ \varepsilon v_t=\nabla^2 v+u-\gamma v & \text{in } \Omega\times(0,T]\end{cases} \tag{P_ε}$$

where

$$f_\varepsilon(u)=u(1-u)(u-1/2+\alpha\varepsilon)$$

and where α and γ are positive constants. The function χ is called the sensitivity function of the chemotactic aggregation. It satisfies $\chi'(v)>0$ for $v>0$. A simple example is the case where $\chi(v)=kv$, with k being a positive constant.

Let us briefly explain a biological background for Problem (P_ε). It is well-known that most biological individuals migrate by random walk and/or by directed movement. A typical example of directed movement is the chemotaxis in which biological individuals move towards higher gradients of some chemical substance. In the case of the aggregation of slime mold, they secrete such chemotactic substance by themselves and passively aggregate; thus chemotaxis works as an aggregating mechanism.

Recent experiments show that bacterial colonies, where individuals migrate by diffusion and chemotaxis and grow by performing cell-division, exhibit very complex spatial patterns.[6] In order to theoretically under-

stand such chemotactic patterns, several mathematical models have been proposed (for instance ref. 24). Problem (P_ε) is a chemotaxis-growth model which describes the motion of individuals when the amount of nutrients is constant. The unknown functions $u(x, t)$ and $v(x, t)$ are respectively the population density of the individuals and the concentration of the chemotactic substance at position $x \in \Omega$ and time $t > 0$.

A chemotaxis model without a growth term was originally proposed by Keller and Segel[17] to describe the initiation of slime mold aggregation where individuals do not grow. A typical property of the solutions is that the density u localizes as a consequence of the chemotactic effect; in particular u may blow up in higher space dimension. We refer in particular to refs. 8, 16, 21, 9, and 15.

Next we describe the behavior of the solution as ε tends to zero. Let $(u_\varepsilon, v_\varepsilon)$ be the solution of Problem (P_ε). Then as ε tends to 0, the functions $(u_\varepsilon, v_\varepsilon)$ are known to converge to (u^0, v^0) on the time interval $[0, T]$ for some $T > 0$, where u^0 is the characteristic function of a moving domain $\Omega_t \subset\subset \Omega$, whose law of motion is related to v^0 via the following free boundary problem (P_0):

$$
\begin{aligned}
&V = -(N-1)\,\kappa + \frac{\partial \chi(v^0)}{\partial n} + c_0 \alpha \qquad \text{on} \quad \Gamma_t = \partial\Omega_t, \quad t \in (0, T] \\
&\Gamma_t|_{t=0} = \Gamma_0 \\
&-\nabla^2 v^0(x, t) + \gamma v^0(x, t) = \begin{cases} 0, & x \in \Omega \backslash \overline{\Omega_t}, \quad t \in [0, T], \\ 1, & x \in \Omega_t, \quad t \in [0, T] \end{cases} \qquad (P_0) \\
&\frac{\partial v^0}{\partial \nu} = 0 \qquad \text{on } \partial\Omega, \quad t \in [0, T]
\end{aligned}
$$

where n is the outward unit normal vector on Γ_t, V is the normal velocity on Γ_t, κ is the mean curvature on Γ_t (positive if Ω_t is convex) and $\overline{\Omega_t}$ denotes the closure of the region Ω_t, namely $\overline{\Omega_t} = \Omega_t \cup \Gamma_t$. The term $c = c_0\alpha = \sqrt{2}\,\alpha$ is the velocity of the traveling front solution $w(x, t) = w(z)$ $(z = x - ct)$ of the one-dimensional scalar reaction-diffusion equation

$$
w_t = w_{xx} + w(1-w)(w - 1/2 + \alpha), \qquad x \in \mathbf{R}, \quad t > 0
$$

with the following boundary conditions at infinity:

$$
w(-\infty, t) = 1 \qquad \text{and} \qquad w(+\infty, t) = 0
$$

A formal derivation of the motion law for Γ_t is presented in ref. 5 and a rigorous convergence proof has been given by Bonami, Hilhorst, Logak, and Mimura[4] in the case where the equation for v is stationary.

The evolution of Γ_t determines the aggregating patterns of the individuals. In the presence of the chemotactic term, one can numerically observe a number of cases where the solution Γ_t loses convexity and develops very complicated patterns, which would not be the case when the function $\chi(v)$ is spatially constant so that the interface motion is driven simply by mean curvature. Therefore one finds that the pattern dynamics developed by Problem (P_ε) depends crucially on the chemotactic term. One of the main purposes of this paper is to show that exactly the same complex spatial patterns can be realized by a system of reaction-diffusion equations without a drift term.

The organization of this paper is as follows. In Section 2, we present a formal derivation of the interface motion equations corresponding to the Eqs. (1.1) and (1.2) and show that the two interface equations are identical. The technique is based on matched asymptotic expansions using the so-called signed distance function, which is found, for example, in Fife.[11]

In Section 3 we numerically compare the motions of interfaces for (1.1) and (1.2) in two space dimensions and show that they are nearly identical, thereby confirming the theoretical prediction made in Section 2 through formal asymptotics. We also present other numerical results for (1.2) showing some interesting behaviors of the interface such as loss of convexity or convergence to a radially symmetric stationary curve, neither of which would happen if the coefficient $h(x)$ in (1.2) is constant.

Finally, in Section 4, we study systems (1.3) and (P_ε) and show, by a formal asymptotic expansion, that their limiting equations as $\varepsilon \to 0$ give rise to nearly the same free boundary problem as (P_0). We also present numerical results for solutions of (1.3) showing formation of rich spatial patterns which closely resemble those known for the chemotaxis-growth model (P_ε).

2. A FORMAL DERIVATION OF THE INTERFACE EQUATION

In this section we present a formal derivation of the equation of motion of interfaces both for the advection-reaction-diffusion equation

$$\varepsilon u_t = \varepsilon \nabla^2 u + \frac{\varepsilon}{h(x)} \nabla h(x) \cdot \nabla u + \frac{1}{\varepsilon} f(u), \qquad x \in \mathbf{R}^N, \quad t > 0 \tag{2.1}$$

and for the reaction-diffusion equation with a spatially inhomogeneous term:

$$\varepsilon u_t = \varepsilon \nabla^2 u + \frac{1}{\varepsilon} h(x)^2 f(u), \qquad x \in \mathbf{R}^N, \quad t > 0 \tag{2.2}$$

Here ε is a small positive parameter and $h(x)$ is a smooth positive function. We assume that $f(u) = -W'(u)$ is a smooth function derived from a

double-well potential $W(u)$ whose local minima lie at $u=0$ and $u=1$. More precisely we assume that $f(0)=f(a)=f(1)=0$, $f'(0)<0$, $f'(a)>0$, $f'(1)<0$ and

$$\int_0^1 f(u)\,du=0$$

The last condition is equivalent to $W(0)=W(1)$, which means that the potential $W(u)$ has equal depth at its two wells.

Using the multi-time scaling method, one finds that the evolution of solutions of (2.1) and that of (2.2) both consist of several stages. To explain what these stages are, let us first consider the special case where $h(x)=$ const., in which case both Eqs. (2.1) and (2.2) reduce to the so-called Allen–Cahn equation

$$\varepsilon u_t=\varepsilon\nabla^2 u+\frac{1}{\varepsilon}f(u)$$

In what follows u^ε will denote a solution of the above equation.

In the first stage (time scale $\tau=t/\varepsilon^2$), which takes place in a very fast time scale, the effect of diffusion is negligible and u^ε evolves according to the ordinary differential equation $du^\varepsilon/d\tau=f(u^\varepsilon)$. Since the potential W is of double-well type, u^ε approaches 0 if $u^\varepsilon(x,0)<a$ and approaches 1 if $u^\varepsilon(x,0)>a$. Accordingly, a sharp internal layer, where the gradient $|\nabla u^\varepsilon|$ is very large, develops between the two regions $\{u\approx 0\}$ and $\{u\approx 1\}$, or, in other words, near the area where $\{x\in\mathbf{R}^N \mid u^\varepsilon(x,0)=a\}$. In what follows we call the set

$$\Gamma^\varepsilon=\bigcup_{t\geqslant 0}(\Gamma_t^\varepsilon\times\{t\}) \tag{2.3}$$

the *interface*, where $\Gamma_t^\varepsilon=\{x\in\mathbf{R}^N \mid u^\varepsilon(x,t)=a\}$. We will also call Γ_t^ε the *interface at time t*.

In the second stage (time scale $\tilde{\tau}=t/\varepsilon$), which takes place in a slower but still relatively fast time scale, the diffusion term $\nabla^2 u^\varepsilon$ near the interface becomes large enough to balance the reaction term. Here the situation differs depending on whether the potential $W(u)$ has equal well-depth at $u=0$ and $u=1$ (that is, the case $W(0)=W(1)$) or not. As Allen and Cahn[2] have observed, if $W(0)\neq W(1)$, then the interface starts to move at a constant normal velocity. On the other hand, if $W(0)=W(1)$ (which is the case treated in the present paper), the interface remains stationary in this time scale.

In the third stage (time scale t), which applies only to the case where $W(0)=W(1)$, the interface starts to move with normal velocity equal to its

mean curvature.[2] Rubinstein, Sternberg and Keller[22] have given a mathematically sound (but not completely rigorous) account of this phenomena. Later more mathematically rigorous proofs have been given by several authors: Xinfu Chen,[7] among others, has given a complete account of the evolution of interfaces from the first to the third stage.

When $h(x)$ is not a constant function, the above-mentioned scenario remains the same up to the second stage except that the normal velocity of the interface for the case $W(0) \neq W(1)$ now has the form $Ch(x)$ with some constant C. A more intriguing difference appears in the third stage. Namely that the normal velocity of the interface (for the case $W(0) = W(1)$) now depends not only on the curvature but also on the gradient of $h(x)$, thus the spatial inhomogeneity of the coefficient of the reaction term gives rise to a drift effect. In what follows we shall derive this law of motion by using the so-called matched asymptotic expansions (see refs. 1, 11, and 22 for a basic idea of this technique).

2.1. Matched Asymptotic Expansions

Let u^ε be a solution of (2.1) or (2.2) and Γ^ε be the interface defined by (2.3). Hereafter, we assume that the interface Γ^ε is smooth and that Γ_t^ε is a smooth closed hypersurface in $\mathbf{R}^N$ without boundaries for each $t \geqslant 0$. We denote by Ω_t^ε the bounded domain in $\mathbf{R}^N$ enclosed by Γ_t^ε.

Let $d^\varepsilon(x, t)$ be the signed distance function to Γ^ε defined by

$$d^\varepsilon(x, t) = \begin{cases} \operatorname{dist}(x, \Gamma_t^\varepsilon), & x \in \mathbf{R}^N \backslash \overline{\Omega_t^\varepsilon} \\ -\operatorname{dist}(x, \Gamma_t^\varepsilon), & x \in \Omega_t^\varepsilon \end{cases} \tag{2.4}$$

Here $\operatorname{dist}(x, \Gamma_t^\varepsilon)$ is the distance from x to the hypersurface Γ_t^ε in $\mathbf{R}^N$. We remark that $d^\varepsilon = 0$ on Γ^ε and $|\nabla d^\varepsilon| = 1$. We assume that d^ε has the expansion

$$d^\varepsilon(x, t) = d_0(x, t) + \varepsilon d_1(x, t) + \varepsilon^2 d_2(x, t) + \cdots$$

and define

$$\Gamma_t = \{x \in \mathbf{R}^N \mid d_0(x, t) = 0\} \tag{2.5}$$

$$\Omega_t = \{x \in \mathbf{R}^N \mid d_0(x, t) < 0\} \tag{2.6}$$

$$\Gamma = \bigcup_{t \geqslant 0} (\Gamma_t \times \{t\}) \tag{2.7}$$

$$Q_0 = \bigcup_{t \geqslant 0} ((\mathbf{R}^N \backslash \overline{\Omega_t}) \times \{t\}) \tag{2.8}$$

$$Q_1 = \bigcup_{t \geqslant 0} (\Omega_t \times \{t\}) \tag{2.9}$$

Roughly speaking, Γ_t represents the position of the interface at time t in the limit as $\varepsilon \to 0$, while Ω_t represents the region inside Γ_t.

We also assume that the solution u^ε has the expansions

$$u^\varepsilon(x, t) = u_0(x, t) + \varepsilon u_1(x, t) + \varepsilon^2 u_2(x, t) + \cdots \tag{2.10}$$

away from the interface Γ^ε (the outer expansion) and

$$u^\varepsilon(x, t) = U_0(\xi, x, t) + \varepsilon U_1(\xi, x, t) + \varepsilon^2 U_2(\xi, x, t) + \cdots \tag{2.11}$$

near Γ^ε (the inner expansion), where $\xi = d^\varepsilon(x, t)/\varepsilon$. The stretched space variable ξ gives exactly the right spatial scaling to describe the sharp transition between the regions $\{u \approx 0\}$ and $\{u \approx 1\}$. Since $u^\varepsilon = a$ on Γ^ε, we normalize U_k in such a way that $U_0(0, x, t) = a$, $U_k(0, x, t) = 0$ $(k = 1, 2, \ldots)$ for all (x, t) near Γ^ε (normalization conditions). To make the inner and outer expansions consistent, we require that

$$U_k(+\infty, x, t) = u_k^+(x, t) \qquad \text{if} \quad x \in (\mathbf{R}^N \backslash \overline{\Omega_t}) \cup \Gamma_t \tag{2.12}$$

$$U_k(-\infty, x, t) = u_k^-(x, t) \qquad \text{if} \quad x \in \Omega_t \cup \Gamma_t \tag{2.13}$$

for all (x, t) near Γ and all $k \geqslant 0$ (matching conditions), where u_k^+ and u_k^- respectively denote the terms of outer expansion (2.10) in the region Q_0 and the region Q_1. In particular, if $x \in \Gamma_t$, then one has to take into account both of the conditions (2.12), (2.13).

2.2. Motion of the Interface for Eq. (2.1)

Substituting the outer expansion (2.10) into (2.1) and collecting the ε^{-1} and ε^0 terms respectively, we get

$$f(u_0(x, t)) = 0$$

$$f'(u_0(x, t))\, u_1(x, t) = 0$$

in $Q_0 \cup Q_1$. The first equation implies $u_0 = 0$, $u_0 = a$ or $u_0 = 1$. Since we are studying interfaces between the regions $\{u \approx 0\}$ and $\{u \approx 1\}$, we have either $u_0(x, t) = 0$ in Q_0 and $u_0(x, t) = 1$ in Q_1 or the other way around. As both cases are treated similarly, we will assume the former throughout this section. From the second condition we get $u_1(x, t) = 0$ in $Q_0 \cup Q_1$.

Next, substituting the inner expansion (2.11) into (2.1) and collecting the ε^{-1} and ε^0 terms, we obtain

$$U_{0\xi\xi} + f(U_0) = 0 \tag{2.14}$$

$$U_{1\xi\xi} + f'(U_0)\, U_1 = U_{0\xi}\left(d_{0t} - \nabla^2 d_0 - \frac{\nabla h \cdot \nabla d_0}{h}\right) - 2\nabla(U_{0\xi}) \cdot \nabla d_0 \tag{2.15}$$

Both (2.14) and (2.15) are ordinary differential equations, with x, t acting the role of parameters. From (2.14) together with the matching conditions and the normalization conditions, we find that

$$U_0(\xi, x, t) = \phi(\xi) \tag{2.16}$$

for all $\xi \in \mathbf{R}$ and all (x, t) near Γ where ϕ is the unique solution of the stationary problem

$$\begin{cases} \phi_{\xi\xi} + f(\phi) = 0, & \xi \in \mathbf{R} \\ \phi(-\infty) = 1, \quad \phi(0) = a, \quad \phi(+\infty) = 0 \end{cases} \tag{2.17}$$

Note that this is a standing wave solution of the one-dimensional diffusion equation

$$u_t = u_{xx} + f(u)$$

See ref. 12 for the details of (2.17).

Substituting (2.16) into (2.15) and recalling the normalization conditions, we get

$$\begin{cases} U_{1\xi\xi} + f'(\phi(\xi))\, U_1 = \left(d_{0t} - \nabla^2 d_0 - \dfrac{\nabla h \cdot \nabla d_0}{h} \right) \phi'(\xi), & \xi \in \mathbf{R} \\ U_1(0, x, t) = 0 \end{cases} \tag{2.18}$$

The following Fredholm type lemma gives us the solvability condition for (2.18), which is a direct consequence of a result proven by Alikakos, Bates and Chen [1, Lemma 4.1].

Lemma 2.1. Let $A(\xi, x, t)$ be given and assume that $A(\xi, x, t) = O(e^{-\delta|\xi|})$ as $|\xi| \to \infty$ for some $\delta > 0$. Then for each (x, t), the following equation

$$\begin{cases} \psi_{\xi\xi} + f'(\phi(\xi))\, \psi = A(\xi, x, t), & \xi \in \mathbf{R} \\ \psi(0, x, t) = 0, \quad \psi(\cdot, x, t) \in L^\infty(\mathbf{R}) \end{cases} \tag{2.19}$$

has a solution if and only if

$$\int_{\mathbf{R}} A(\xi, x, t)\, \phi'(\xi)\, d\xi = 0$$

In addition, the solution, if it exists, is unique and satisfies $\psi(\xi, x, t) = O(e^{-\delta|\xi|})$ as $|\xi| \to \infty$.

By this lemma, the solvability condition for (2.18) yields

$$d_{0t} = \nabla^2 d_0 + \frac{\nabla h \cdot \nabla d_0}{h}$$

and thus $U_1(\xi, x, t) = 0$ for all $\xi \in \mathbf{R}$. (Incidentally, this U_1 satisfies the matching conditions (2.12) and (2.13)).

Let us derive the equation of interface motion from (2.20). Since ∇d_0 $(= \nabla_x d_0(x, t))$ coincides with the outward normal unit vector to the hypersurface Γ_t, one easily sees that $-d_{0t}(x, t) = V$, where V is the normal velocity of the interface Γ_t. It is also known that the mean curvature κ of the interface is equal to $-\nabla^2 d_0/(N-1)$. Thus Eq. (2.20) is equivalent to

$$V = -(N-1)\,\kappa - \frac{\partial}{\partial n}(\log h) \qquad \text{on } \Gamma_t \tag{2.20}$$

2.3. Motion of the Interface for Eq. (2.2)

Substituting the outer expansion (2.10) into (2.2) and collecting the ε^{-1} and ε^0 terms respectively, we get

$$h(x)^2 f(u_0(x, t)) = 0$$
$$h(x)^2 f'(u_0(x, t))\, u_1(x, t) = 0$$

in $Q_0 \cup Q_1$. Hence we have $u_0(x, t) = 0$ in Q_0, $u_0(x, t) = 1$ in Q_1 and $u_1(x, t) = 0$ in $Q_0 \cup Q_1$.

Substituting the inner expansion (2.11) into (2.2) and collecting the ε^{-1} and ε^0 terms, we get

$$U_{0\xi\xi} + h(x)^2 f(U_0) = 0 \tag{2.21}$$
$$U_{1\xi\xi} + h(x)^2 f'(U_0)\, U_1 = U_{0\xi}(d_{0t} - \nabla^2 d_0) - 2\nabla(U_{0\xi}) \cdot \nabla d_0 \tag{2.22}$$

From (2.21) together with the matching conditions and the normalization conditions,

$$U_0(\xi, x, t) = \phi(h(x)\,\xi) \tag{2.23}$$

for all $\xi \in \mathbf{R}$ and all (x, t) near Γ where ϕ is the solution of (2.17). Then Eq. (2.22) becomes

$$\begin{aligned} &U_{1\xi\xi} + h(x)^2 f'(\phi(h(x)\,\xi))\, U_1 \\ &\quad = (d_{0t} - \nabla^2 d_0)\, h(x)\, \phi'(h(x)\,\xi) \\ &\qquad - 2\nabla h \cdot \nabla d_0 \{\phi'(h(x)\,\xi) + h(x)\,\xi\phi''(h(x)\,\xi)\}, \qquad \xi \in \mathbf{R} \end{aligned}$$

Letting $z = h(x)\,\xi$ and taking into consideration the normalization conditions, we have

$$\begin{cases} U_{1zz} + f'(\phi(z))\,U_1 = \left(d_{0t} - \nabla^2 d_0 - \dfrac{2\nabla h \cdot \nabla d_0}{h}\right)\dfrac{\phi'(z)}{h} - \dfrac{2\nabla h \cdot \nabla d_0}{h^2}\,z\phi''(z) \\ U_1(0, x, t) = 0 \end{cases} \tag{2.24}$$

The solvability condition for (2.24) is written as

$$\left(d_{0t} - \nabla^2 d_0 - \frac{2\nabla h \cdot \nabla d_0}{h}\right)\int_{\mathbf{R}} \{\phi'(z)\}^2\,dz - \frac{2\nabla h \cdot \nabla d_0}{h}\int_{\mathbf{R}} z\phi'(z)\,\phi''(z)\,dz = 0$$

Using $\int_{\mathbf{R}} z\phi'\phi''\,dz = -\frac{1}{2}\int_{\mathbf{R}} (\phi')^2\,dz$, we get

$$d_{0t} = \nabla^2 d_0 + \frac{\nabla h \cdot \nabla d_0}{h}$$

thus again the interface equation (2.20). Incidentally, we have

$$U_1(\xi, x, t) = \frac{\nabla h \cdot \nabla d_0}{h^2}\,\Psi(h(x)\,\xi)$$

where $\Psi(z)$ is the unique solution of

$$\begin{cases} \Psi_{zz} + f'(\phi(z))\,\Psi = -(\phi'(z) + 2z\phi''(z)), & z \in \mathbf{R} \\ \Psi(0) = 0, \qquad \Psi \in L^\infty(\mathbf{R}) \end{cases}$$

In conclusion, we have formally proven that as $\varepsilon \to 0$, solutions u^ε of Eq. (2.1) and those of (2.2) both satisfy

$$u^\varepsilon \to \begin{cases} 0, & x \in \mathbf{R}^N \backslash \overline{\Omega_t} \\ 1, & x \in \Omega_t \end{cases}$$

where the boundary Γ_t of Ω_t moves according to the law (2.20).

It is perhaps useful to note that the interface equation (2.20) can be derived from the interface energy

$$\int_0^1 \sqrt{2(W(u) - W(0))}\,du \int_{\Gamma_t} h(x)\,dS_x$$

which is obtained by letting $\varepsilon \to 0$ in the free energy

$$\int_{\mathbf{R}^N} \left\{\frac{\varepsilon}{2}|\nabla u|^2 + \frac{h(x)^2}{\varepsilon}(W(u) - W(0))\right\} dx \tag{2.25}$$

See refs. 18 and 23 for derivation of (2.25) as a singular limit of the above energy.

3. NUMERICAL SIMULATIONS IN A SQUARE REGION IN $\mathbf{R}^2$

In this section we numerically investigate the dynamics of solutions of (2.1) and (2.2) for $N=2$. Recall that both of these equations have the same interface equation (2.20) in the singular limit as $\varepsilon \to 0$.

If h is a constant function, then the interface equation becomes what is called the curve shortening equation

$$V = -\kappa \tag{3.1}$$

The motion of curves according to (3.1) is well understood. The results of Gage and Hamilton[13] and Grayson[14] imply that the solution of (3.1) starting from any non-self-intersecting closed curve Γ_0 becomes convex and shrinks to a single point in finite time.

For computational simplicity, the domain will be restricted to a square region $\Omega = \{(x, y) \in \mathbf{R}^2 \mid 0 < x < l, 0 < y < l\}$ with the zero-flux boundary conditions on the boundary $\partial\Omega$. In the following figures, the white region approximately represents the set Ω_t^ε and the black region approximately represents $\Omega \backslash \overline{\Omega_t^\varepsilon}$.

3.1. Stable Stationary Solutions

3.1.1. Radial Case. Suppose that the function h is radially symmetric, so that one can write $h = h(r)$. In this situation, if the initial curve Γ_0 is a circle with center at the origin, then Γ_t remains a circle for each $t > 0$. Let $R(t)$ be the radius of Γ_t. Then Eq. (2.20) is equivalent to

$$\frac{dR}{dt} = -\frac{1}{R} - \frac{h'(R)}{h(R)} = -\frac{d}{dR}\log(Rh(R)) \tag{3.2}$$

Therefore if $Rh(R)$ attains a local minimum, say at $R = R^*$, then the circular interface with radius R^* is a stationary solution and is stable with respect to any radially symmetric perturbation. It then follows from the comparison theorem that this stationary interface is also stable with respect to any perturbation.

To prove this last statement, let Γ_0 be a closed curve obtained by giving a small—but not necessarily radially symmetric—perturbation to the circle $r = R^*$. Then Γ_0 is enclosed between the circles $r = R^* - \delta$ and $r = R^* + \delta$, where δ is very small. Let $\Gamma_-(t)$, $\Gamma(t)$, $\Gamma_+(t)$ be the solutions of the

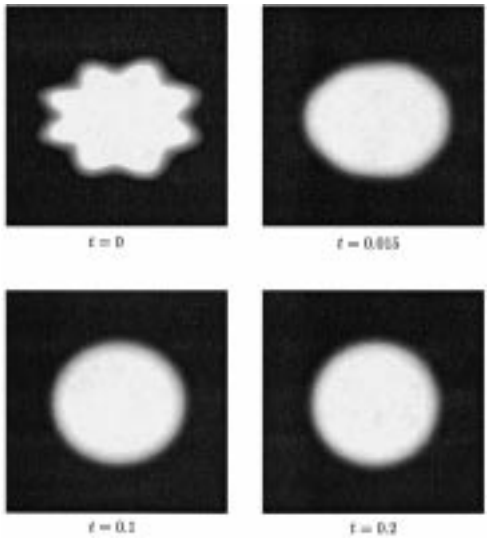

Fig. 1. Time evolution of $u^\varepsilon(x, t)$ of (2.1) when $\varepsilon = 0.025$, $f(u) = u(1-u)(u-1/2)$ and $h(x) = 1/(|x|^2 + 1/9) + 1$.

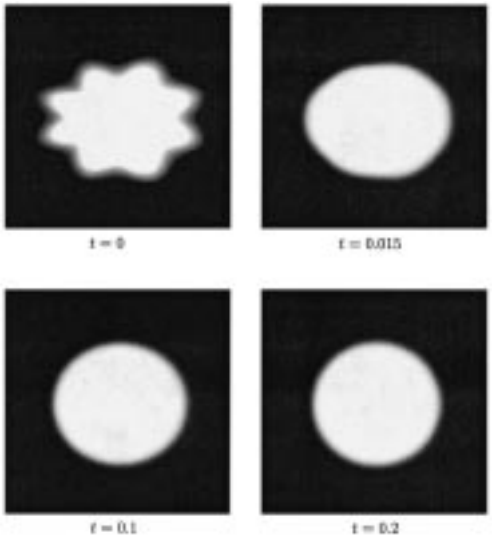

Fig. 2. Time evolution of $u^\varepsilon(x, t)$ of (2.2) where ε, f, h are the same as in Fig. 1.

interface equation (2.20) for the initial data $r = R^* - \delta$, Γ_0 and $r = R^* + \delta$, respectively. By the stability of the circle $r = R^*$ with respect to radially symmetric perturbations, the two circles $\Gamma_-(t)$, $\Gamma_+(t)$ remain close to the circle $r = R^*$ as time passes. And, by the comparison theorem, the curve $\Gamma(t)$ remains enclosed between the circles $\Gamma_-(t)$, $\Gamma_+(t)$. Consequently, the curve $\Gamma(t)$ remains close to the circle $r = R^*$, which proves the stability of this circle with respect to arbitrary small perturbations.

Figures 1 and 2 show convergence of an arbitrarily chosen interface to such a stable circular interface in the case where $h(x) = 1/(|x|^2 + 1/9) + 1$. In this case, $R^* = \sqrt{5}/3$. Figure 1 shows the interface motion for Eq. (2.1) and Fig. 2 that for Eq. (2.2) with $\varepsilon = 0.025$.

As anticipated from the fact that Eqs. (2.1) and (2.2) share the same limit interface equation (2.20), we observe very similar interface motion in Figs. 1 and 2. Note, however, that there is difference between the thickness of the internal layer around the interface for Eq. (2.1) and that for Eq. (2.2)—a fact reflected by the difference of the U_0 terms (2.16) and (2.23).

3.1.2. Nonradial case. Figures 3 and 4 respectively show the behaviors of interfaces for Eqs. (2.1), (2.2) when $h(x) = \exp(1.25 \cos(3(4x_1^2 + x_2^2)))$ and the initial interface is circular. Again the motions of the two interfaces are nearly identical, and they approach a stable ellipse-like curve.

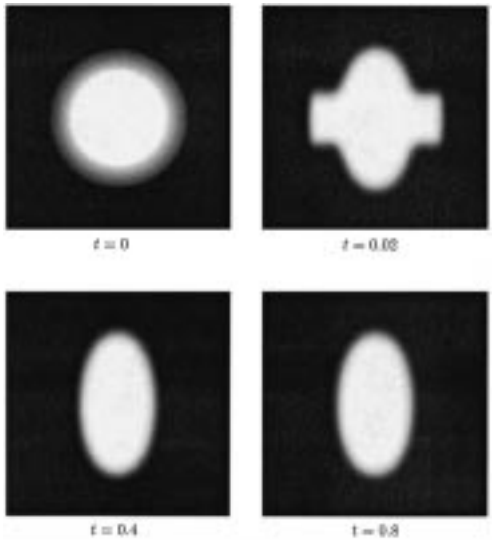

Fig. 3. Time evolution of $u^\varepsilon(x, t)$ of (2.1) when $\varepsilon = 0.025$, $f(u) = u(1-u)(u-1/2)$ and $h(x) = \exp(p \cos(q(4x_1^2 + x_2^2)))$ with $p = 1.25$, $q = 3$.

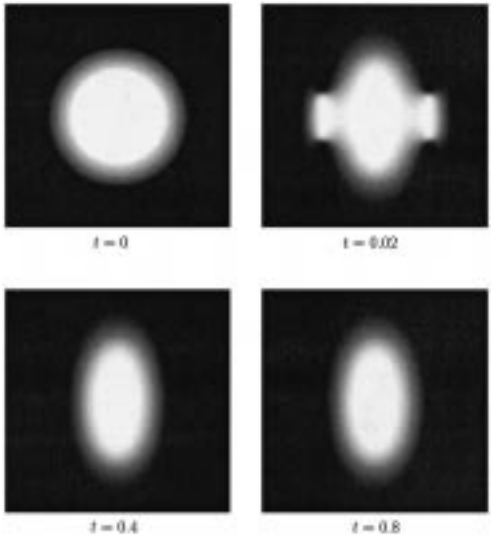

Fig. 4. Time evolution of $u^\varepsilon(x, t)$ of (2.2) where ε, f, h are the same as in Fig. 3.

3.2. Loss of Convexity

An initially convex interface may lose its convexity in finite time even if $h(x)$ has convex level curves, as already observed in Figs. 3 and 4. Loss of convexity occurs even when $h(x)$ is radially symmetric. Figures 5 and 6 —respectively for Eqs. (2.1) and (2.2)—show such an example.

4. MOTION OF THE INTERFACE FOR A REACTION-DIFFUSION SYSTEM

In this section we introduce a reaction-diffusion system without a drift term:

$$\begin{cases} \varepsilon u_t = \varepsilon \nabla^2 u + \dfrac{1}{\varepsilon} h(v)^2 f_\varepsilon(u), & x \in \mathbf{R}^N, \quad t > 0 \\ \varepsilon v_t = \nabla^2 v + u - \gamma v, & x \in \mathbf{R}^N, \quad t > 0 \end{cases} \tag{4.1}$$

where $f_\varepsilon(u) = u(1-u)(u-1/2+\alpha\varepsilon)$. Our purpose is to show, by formal asymptotics, that the motion of interface for this equation is nearly identical to that for the so-called chemotaxis-growth system

$$\begin{cases} \varepsilon u_t = \varepsilon \nabla^2 u - \varepsilon \nabla \cdot (u \nabla \chi(v)) + \dfrac{1}{\varepsilon} f_\varepsilon(u), & x \in \mathbf{R}^N, \quad t > 0 \\ \varepsilon v_t = \nabla^2 v + u - \gamma v, & x \in \mathbf{R}^N, \quad t > 0 \end{cases} \tag{4.2}$$

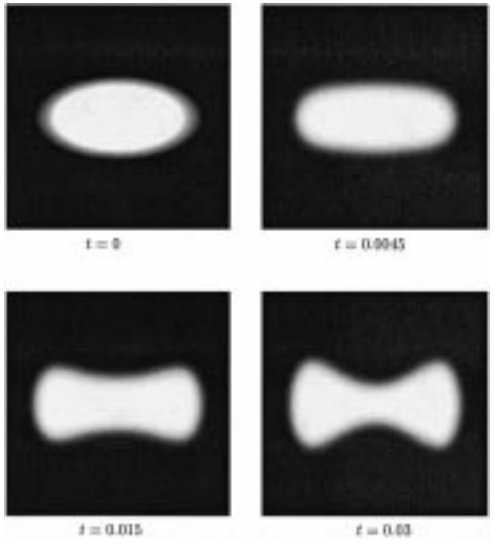

Fig. 5. Time evolution of $u^\varepsilon(x, t)$ of (2.1) when $\varepsilon = 0.025$, $f(u) = u(1-u)(u-1/2)$ and $h(x) = \exp(p \sin(q\pi |x|^2)$ with $p = 1.956$, $q = 1.15$.

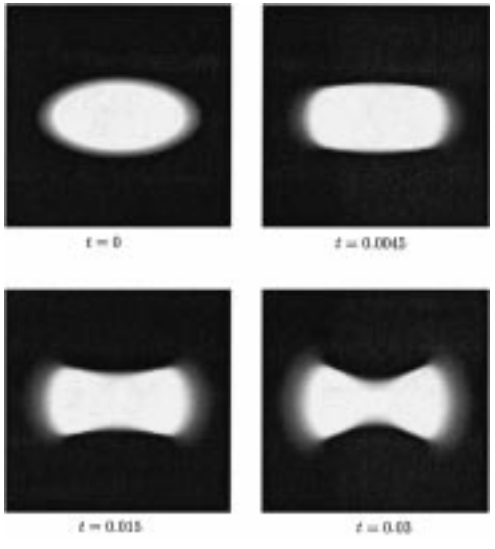

Fig. 6. Time evolution of $u^\varepsilon(x, t)$ of (2.2) where ε, f, h are the same as in Fig. 5.

which has been proposed by ref. 19 as a model of aggregating biological individuals in the case where $h(v) = e^{-\chi(v)}$. We will then present numerical results that show some interesting aggregating patterns for (4.1).

Let $(u^\varepsilon, v^\varepsilon)$ be the solution of (4.1) or (4.2). As before, we define the interface Γ^ε by

$$\Gamma^\varepsilon = \bigcup_{t \geqslant 0} (\Gamma_t^\varepsilon \times \{t\})$$

where $\Gamma_t^\varepsilon = \{(x, t) \mid u^\varepsilon(x, t) = 1/2\}$. We also define $d_0(x, t)$, Γ_t, Ω_t, Γ, Q_0 and Q_1 as in Section 2.

By letting $\varepsilon \to 0$ in (4.2), Bonami, Hilhorst, Logak and Mimura[5] have formally derived the following free boundary problem which describes the law of interface motion for the chemotaxis-growth model:

$$\begin{aligned} &V = -(N-1)\kappa + \frac{\partial \chi(v_0)}{\partial n} + \sqrt{2}\,\alpha \qquad \text{on } \Gamma_t \\ &-\nabla^2 v_0 + \gamma v_0 = \begin{cases} 0, & x \in \mathbf{R}^N \backslash \overline{\Omega_t}, \\ 1, & x \in \Omega_t \end{cases} \end{aligned} \tag{4.3}$$

Their derivation is based upon using the traveling wave of an auxiliary problem and the signed distance function as it is done, for example, by Barles, Soner and Souganidis.[3] We remark that this method is for the most part equivalent to the method of matched asymptotic expansions which we have explained in Section 2. Bonami *et al.* have also given a rigorous convergence proof in the case where the equation for v is stationary.[4]

We now formally derive a free boundary problem for our model (4.1) by using matched asymptotic expansions. We assume that u^ε has the outer expansion (2.10) and the inner expansion (2.11) and we impose the same normalization conditions and matching conditions as in Section 2.1. We also assume that v^ε has the expansion

$$v^\varepsilon(x, t) = v_0(x, t) + \varepsilon v_1(x, t) + \varepsilon^2 v_2(x, t) + \cdots \tag{4.4}$$

for all (x, t).

Substituting (2.10) and (4.4) into (4.1) and collecting the ε^{-1} and ε^0 terms, we get

$$h(v_0)^2 f_0(u_0) = 0 \tag{4.5}$$

$$2h(v_0) h'(v_0) v_1 f_0(u_0) + h(v_0)^2 f_0'(u_0) u_1 + h(v_0)^2 f_1(u_0) = 0 \tag{4.6}$$

$$\nabla^2 v_0 + u_0 - \gamma v_0 = 0 \tag{4.7}$$

in $Q_0 \cup Q_1$, where $f_0(u) = u(1-u)(u-1/2)$ and $f_1(u) = \alpha u(1-u)$. By (4.5) and (4.6), we have $u_0(x, t) = 0$ in Q_0, $u_0(x, t) = 1$ in Q_1 and $u_1(x, t) = 0$ in $Q_0 \cup Q_1$ independently of the values of $v_0(x, t)$ and $v_1(x, t)$. Hence by (4.7), v_0 is the solution of

$$-\nabla^2 v_0 + \gamma v_0 = \begin{cases} 0, & x \in \mathbf{R}^N \backslash \overline{\Omega_t} \\ 1, & x \in \Omega_t \end{cases} \tag{4.8}$$

Substituting (2.11) and (4.4) into the first equation of (4.1) and collecting the ε^{-1} and ε^0 terms, we get

$$U_{0\xi\xi} + h(v_0)^2 f_0(U_0) = 0 \tag{4.9}$$

$$\begin{aligned} U_{1\xi\xi} + h(v_0)^2 f_0'(U_0)\, U_1 = {} & U_{0\xi}(d_{0t} - \nabla^2 d_0) - 2\nabla(U_{0\xi}) \cdot \nabla d_0 \\ & - 2h(v_0) h'(v_0) v_1 f_0(U_0) - h(v_0)^2 f_1(U_0) \end{aligned} \tag{4.10}$$

It follows from (4.9), the matching conditions and the normalization conditions that

$$U_0(\xi, x, t) = \phi(h(v_0(x, t))\, \xi)$$

for all $\xi \in \mathbf{R}$ and all (x, t) near Γ, where ϕ is the solution of (2.17) with $f = f_0$, namely

$$\phi(\xi) = \frac{1}{2}\left(1 - \tanh\left(\frac{\xi}{2\sqrt{2}}\right)\right)$$

Letting $z = h(v_0(x, t))\, \xi$, we obtain from (4.10)

$$\begin{aligned} U_{1zz} + f_0'(\phi(z))\, U_1 = {} & \frac{1}{h(v_0)} (d_{0t} - \nabla^2 d_0)\, \phi'(z) \\ & - 2\frac{h'(v_0)}{h(v_0)^2} \nabla v_0 \cdot \nabla d_0 (\phi'(z) + z\phi''(z)) \\ & - 2\frac{h'(v_0)}{h(v_0)} v_1 f_0(\phi(z)) - f_1(\phi(z)) \end{aligned} \tag{4.11}$$

The solvability condition for (4.11) with the normalization conditions implies

$$\left(d_{0t}-\nabla^2 d_0-2\frac{h'(v_0)}{h(v_0)}\nabla v_0\cdot\nabla d_0\right)\int_{\mathbf{R}}\{\phi'(z)\}^2\,dz$$
$$-2\frac{h'(v_0)}{h(v_0)}\nabla v_0\cdot\nabla d_0\int_{\mathbf{R}} z\phi'(z)\,\phi''(z)\,dz-2h'(v_0)\,v_1\int_{\mathbf{R}} f_0(\phi(z))\,\phi'(z)\,dz$$
$$-h(v_0)\int_{\mathbf{R}} f_1(\phi(z))\,\phi'(z)\,dz=0 \tag{4.12}$$

Note that the function ϕ also satisfies

$$\phi''+c\phi'+f_\varepsilon(\phi)=0,\qquad z\in\mathbf{R} \tag{4.13}$$

with $c=\sqrt{2}\,\alpha\varepsilon$. Multiplying (4.13) by ϕ' and integrating over $\mathbf{R}$, we get

$$\int_{\mathbf{R}} f_1(\phi(z))\,\phi'(z)\,dz=-\sqrt{2}\,\alpha\int_{\mathbf{R}}\{\phi'(z)\}^2\,dz$$

Therefore we obtain from (4.12)

$$d_{0t}=\nabla^2 d_0+\frac{h'(v_0)}{h(v_0)}\nabla v_0\cdot\nabla d_0-\sqrt{2}\,\alpha h(v_0)$$

Letting $\chi(v)=-\log h(v)$, we have formally proven that the interface Γ_t moves according to the following free boundary problem, which is very similar to (4.3):

$$\begin{aligned} &V=-(N-1)\,\kappa+\frac{\partial\chi(v_0)}{\partial n}+\sqrt{2}\,\alpha e^{-\chi(v_0)} \qquad \text{on } \Gamma_t\\ &-\nabla^2 v_0+\gamma v_0=\begin{cases}0, & x\in\mathbf{R}^N\backslash\overline{\Omega_t}\\ 1, & x\in\Omega_t\end{cases}\end{aligned} \tag{4.14}$$

Remark 4.1. When the constant α depends on v and is given by $\alpha=\tilde{\alpha}e^{\chi(v)}$, the free boundary problem (4.14) completely coincides with (4.3).

In ref. 19, Mimura and Tsujikawa have studied the existence and stability of radially symmetric stationary solutions to a variant of (4.2), namely

$$\begin{cases}u_t=\varepsilon^2\nabla^2 u-\varepsilon\nabla\cdot(u\nabla\chi(v))+f(u), & x\in\Omega,\quad t>0\\ v_t=\nabla^2 v+u-\gamma v, & x\in\Omega,\quad t>0\end{cases} \tag{4.15}$$

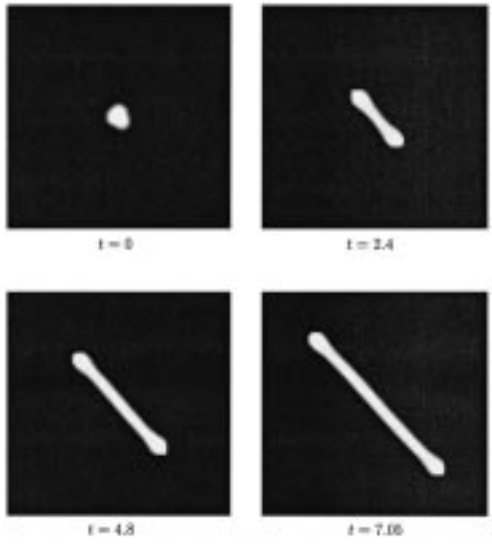

Fig. 7. Time evolution of $u^{\varepsilon}(x, t)$ of (4.1) when $\varepsilon = 0.05$, $\alpha = 1.0$, $\gamma = 1.0$, $h(v) = a \exp(-bv)$ with $a = 20/\sqrt{2}$, $b = 6.41$.

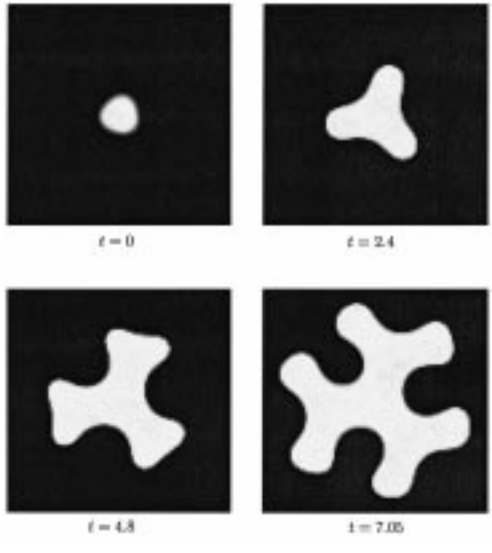

Fig. 8. Time evolution of $u^{\varepsilon}(x, t)$ of (4.1) when $\varepsilon = 0.05$, $\alpha = 1.0$, $\gamma = 5.0$, $h(v) = a \exp(-bv)$ with $a = 20/\sqrt{2}$, $b = 17.55$.

and have numerically observed highly complex aggregating patterns (see also ref. 20). As shown in Figs. 7 and 8 below, we also observe very similar complex spatial patterns for our model.

In Fig. 7, parameters are chosen so that planar interfaces are stable and the circular stationary interface has 2-mode instability. One observes that an originally circular interface eventually becomes a rod-shaped pattern which stretches at a constant speed.

In Fig. 8, parameters are chosen so that planar interfaces are stable and the circular stationary interface has 3-mode instability. One observes triangularly branching patterns.

Both of the patterns observed in Figs. 7, 8 closely resemble those found in ref. 19.

REFERENCES

1. N. D. Alikakos, P. W. Bates, and X. Chen, Convergence of the Cahn–Hilliard equation to the Hele–Shaw model, *Arch. Rational Mech. Anal.* **128**:165–205 (1994).
2. S. Allen and J. Cahn, A microscopic theory for antiphase boundary motion and its application to antiphase domain coarsening, *Acta Metall.* **27**:1084–1095 (1979).
3. G. Barles, H. M. Soner, and P. E. Souganidis, Front propagation and phase field theory, *SIAM J. Control Optim.* **31**:439–469 (1993).
4. A. Bonami, D. Hilhorst, E. Logak, and M. Mimura, Singular limit of a chemotaxis-growth model, preprint.
5. A. Bonami, D. Hilhorst, E. Logak, and M. Mimura, A free boundary problem arising in a chemotaxis model, *Free Boundary Problems, Theory and Applications*, M. Niezgódka and P. Strzelecki, eds., Pitman Res. Notes in Math. Series **363** (1996).
6. E. O. Budrene and H. C. Berg, Complex patterns formed by motile cells of Escherichia coli, *Nature* **349**:630–633 (1991).
7. X. Chen, Generation and Propagation of Interfaces for Reaction-Diffusion Equations, *J. Differential Equations* **96**:116–141 (1992).
8. S. Childress and J. K. Percus, Nonlinear aspects of chemotaxis, *Math. Biosci.* **56**:217–237 (1986).
9. J. I. Diaz and T. Nagai, Symmetrization in a parabolic-elliptic system related to chemotaxis, *Advances in Math. Sciences and Appl.* **5**:659–680 (1995).
10. L. C. Evans, H. M. Soner, and P. E. Souganidis, Phase transitions and generalized motion by mean curvature, *Comm. Pure Appl. Math.* **45**:1097–1123 (1992).
11. P. C. Fife, "Dynamics of Internal Layers and Diffusive Interfaces," CBMS-NSF Regional Conf. Ser. in Appl. Math., SIAM, Philadelphia (1988).
12. P. C. Fife and J. B. McLeod, The Approach of Solutions of Nonlinear Diffusion Equations to Travelling Front Solutions, *Arch. Rational Mech. Anal.* **65**:335–361 (1977).
13. M. Gage and R. S. Hamilton, The heat equation shrinking convex plane curves, *J. Differential Geom.* **23**:69–96 (1986).
14. M. A. Grayson, The heat equation shrinks embedded plane curves to round points, *J. Differential Geom.* **26**:285–314 (1987).
15. M. A. Herrero and J. J. L. Velázquez, Chemotactic collapse for the Keller–Segel model, *J. Math. Biol.* **35**:177–194 (1996).

16. W. Jäger and S. Luckhaus, On explosions of solutions to a system of partial differential equations modelling chemotaxis, *Trans Amer. Math. Soc.* **329**:819–824 (1992).
17. E. F. Keller and L. A. Segel, Initiation of slime mold aggregation viewed as an instability, *J. Theor. Biol.* **26**:399–415 (1970).
18. R. V. Kohn and P. Sternberg, Local minimisers and singular perturbations, *Proc. Roy. Soc. Edinburgh*, **111A**:69–84 (1989).
19. M. Mimura and T. Tsujikawa, Aggregating pattern dynamics in a chemotaxis model including growth, *Physica A* **230**:499–543 (1996).
20. M. Mimura, T. Tsujikawa, R. Kobayashi, and D. Ueyama, Dynamics of aggregation patterns in a chemotaxis-diffusion-growth model equation, *Forma* **8**:179–195 (1993).
21. T. Nagai, Blow-up of radially symmetric solutions to a chemotaxis system, *Advances in Math. Sciences and Appl.* **5**:581–601 (1995).
22. J. Rubinstein, P. Sternberg, and J. B. Keller, Fast reaction, slow diffusion and curve shortening, *SIAM J. Appl. Math.* **49**:116–133 (1989).
23. P. Sternberg, The effect of a singular perturbation on nonconvex variational problems, *Arch. Rational Mech. Anal.* **101**:209–260 (1988).
24. D. E. Woodward, J. Tyson, M. R. Myerscough, J. D. Murray, E. O. Budrene, and H. C. Berg, Spatio-temporal patterns generated by Salmonella typhymerium, *Biophys.* **68**:2181–2189 (1995).